(9) Kitaigorodskii, A. I. "Organic Chemical Crystallography"; Consultant's Bureau: New York, 1961; p 231.
(10) Kitaigorodskii, A. I. "Molecular Crystals and Molecules"; Academic Press: New York, 1973; p 116.
(11) Mnyukh, Yu. V. *Zh. Strukt. Khim* **1960**, *1*, 370.
(12) Teare, P. W. *Acta Crystallogr.* **1959**, *12*, 294.
(13) Shearer, H. M. M.; Vand, V. *Acta Crystallogr.* **1956**, *9*, 379.
(14) Piesczek, W.; Strobl, G. R.; Malzahn, K. *Acta Crystallogr. Sect. B: Struct. Crystallogr. Cryst. Chem.* **1974**, *B30*, 1278.
(15) Wittmann, J. C.; Hodge, A. M.; Lotz, B. *J. Polym. Sci., Polym. Phys. Ed.* **1983**, *21*, 2495.
(16) Amoros, J. L.; Amoros, M. "Molecular Crystals. Their Transforms and Diffuse Scattering"; Wiley: New York, 1968.
(17) Doyle, P. A.; Turner, P. S. *Acta Crystallogr. Sect. A: Cryst. Phys., Diffr., Gen. Crystallogr.* **1968**, *A24*, 390.
(18) Cowley, J. M. "Diffraction Physics", 2nd ed.; North Holland: Amsterdam, 1981; p 238ff.
(19) Müller, A. *Proc. R. Soc. London, A* **1932**, *138*, 514.
(20) Maroncelli, M.; Qi, S. P.; Strauss, H. L.; Synder, R. G. *J. Am. Chem. Soc.* **1982**, *104*, 6237.
(21) Moss, B.; Dorset, D. L.; Wittmann, J. C.; Lotz, B. *J. Polym. Sci., Polym. Phys. Ed.* **1984**, *22*, 1919.
(22) Azaroff, L. V. "Introduction to Solids"; McGraw-Hill: New York, 1960; pp 186ff.
(23) Ungar, G.; Keller, A. *Colloid Polym. Sci.* **1979**, *257*, 90.
(24) Zerbi, G.; Piazza, R.; Holland-Moritz, K. *Polymer* **1982**, *23*, 1921.
(25) Smith, A. E. *J. Chem. Phys.* **1953**, *21*, 2229.
(26) Dorset, D. L.; Moss, B.; Wittmann, J. C.; Lotz, B. *Proc. Natl. Acad. Sci. U.S.A.* **1984**, *81*, 1913.
(27) Dorset, D. L.; Moss, B.; Zemlin, F. *J. Macromol. Sci. Phys.*, in press.
(28) Strobl, G.; Ewen, B.; Fischer, E. W.; Piesczek, W. *J. Chem. Phys.* **1974**, *61*, 5257.
(29) Smith, P.; Manley, R. St. J. *Macromolecules* **1979**, *12*, 483.
(30) Wunderlich, B. "Macromolecular Physics, Crystal Melting"; Academic Press: New York, 1980; Vol. 3, p 83ff.
(31) Sawzik, P. Ph.D. Thesis, University of Pittsburgh, Pittsburgh, PA, 1984.
(32) Ubbelohde, A. R. "The Molten State of Matter"; Wiley: New York, 1978; Chapter 4.
(33) Nyburg, S. C.; Potoworowski, J. A. *Acta Crystallogr., Sect. B: Struct. Crystallogr. Cryst. Chem.* **1973**, *B29*, 347.

Influence of the Head-to-Head Defect and the Molecular Weight on the $\alpha \rightarrow \gamma$ Solid-State Transformation of Poly(vinylidene fluoride)

Lien Tai Chen and Curtis W. Frank*

Department of Chemical Engineering, Stanford University, Stanford, California 94305.
Received June 4, 1984

ABSTRACT: Crystallization of PVF_2 from the melt results in three peaks in the melting endotherm obtained by differential scanning calorimetry; these correspond to α, crystallized γ, and transformed γ forms. An additional low-melting peak is attributed to the interlamellar crystallization that occurs during quenching. Areas of these peaks are determined and used to study the solid-state $\alpha \rightarrow \gamma$ transformation. The extent of the transformation appears to increase with the percentage of the γ spherulites in the crystalline regions but to decrease with the content of the interlamellar amorphous layers. The results support Lovinger's proposal that the transformation proceeds more rapidly in the longitudinal direction toward the α-nuclei than in the transverse direction. Moreover, the two competing factors—the percentage of the γ spherulites and the interlamellar amorphous content—increase with either the reversed monomer (head-to-head defect) content or the molecular weight. As a result, the $\alpha \rightarrow \gamma$ transformation is a complex function of the head-to-head defect concentration and the molecular weight.

Introduction

Poly(vinylidene fluoride) (PVF_2) has been extensively studied and much is known about the morphological and electrical characteristics.[1] The focus of this work is on the α and γ polymorphs that are formed upon crystallization from the melt.[2] In particular, we wish to examine the influence of the reversed monomer content, or head-to-head (H/H) defect, and the molecular weight on the solid-state $\alpha \rightarrow \gamma$ transformation. This transformation is of interest because the α form, containing two molecular chains of TGTG′ conformation in the unit cell, is nonpolar, whereas the γ form, containing two chains of TTTGTTTG′ conformation, is polar. Thus, high-temperature annealing could potentially be used to transform a piezoelectrically inactive sample into a piezoelectrically active one.

Prest and Luca[3] were the first to report on the $\alpha \rightarrow \gamma$ solid-state transformation in a study employing differential scanning calorimetry and infrared spectroscopy. Proposals for the molecular mechanism have been made by Takahashi and Tadokoro[4] and by Lovinger.[5] In addition, Lovinger[6] has also suggested a bulk mechanism involving the morphological superstructure. A major objective of this paper is to provide quantitative verification of Lovinger's[6] proposal through application of differential scanning calorimetry to well-characterized commercial samples of PVF_2.

Table I
Area Ratios from Differential Scanning Calorimetry Melting Endotherms Used in the Correlations in Figures 2–7

sample	H/H defect content	mol wt	$A_p/(A_\alpha+A_{\gamma'})$	$A_{\gamma'}/(A_\alpha+A_{\gamma'})$	$A_{\gamma'}/(A_\alpha+A_\gamma+A_{\gamma'})$
SU 53	3.3	140 000	0.0	1.9	2.6
SU 51	3.6	130 000	0.0	2.1	0.8
Solvay 537	4.0	52 000	0.0	1.2	2.1
Solef 1012	4.0	222 000	9.4	0.0	1.8
Dyflor 2000E	4.2	135 000	2.4	2.4	2.1
Solef 1008	4.2	101 000	6.2	5.6	5.6
Solvay 671	4.4	703 000	22.5	5.4	12.8
Solef 1010	4.5	146 000	7.1	5.2	4.8
Dyflor 2000L	5.1	94 000	14.3	2.1	4.7
Kynar 880	5.3	186 000	25.7	2.9	4.8
Dyflor 2000H	5.3	207 000	24.7	9.7	22.5

0024-9297/85/2218-2163$01.50/0

Experimental Section

Two samples synthesized in our laboratory[9] and nine commercial samples, which are listed in Table I, were investigated. Samples were purified by reprecipitation and characterized in a previous study.[7] Each sample was heated to 500 K for 10 min in a Perkin-Elmer DSC-II differential scanning calorimeter (DSC) to ensure melting. This temperature is higher than all reported values of melting temperatures for PVF_2. After crystallization at a predetermined temperature for 24 h, the melting endotherms were obtained with the DSC heating rate set at 10 K/min. The melting temperatures of the crystalline forms were recorded and the peak areas, which are proportional to the content of the corresponding crystalline modifications, were measured by a cutting and weighing technique.

Results and Discussion

Background on the $\alpha \rightarrow \gamma$ Transformation. Since the observation of the $\alpha \rightarrow \gamma$ transformation of PVF_2 by Prest and Luca,[3] a number of papers[4,5,10] have contributed to the understanding of the conformational transition. The α form has a TGTG′ conformation while the γ form has a TTTGTTTG′ conformation. The transition between the two conformations requires bond rotation for an interchange between G or G′ and T. The detailed structures of the two polymorphs have been under consideration recently.

On the one hand, Takahashi and Tadokoro[4] observed diffuse streaks on the X-ray diagram of the α form and attributed them to kink bands in the crystallites that involve TTT conformations. In other words, defects with the γ conformation exist in the α chains. The intensity distribution calculation suggested that the kink bands were one monomeric unit thick and were mainly formed by a flip-flop motion between the TGTG′ and TG′TG conformations.

On the other hand, Lovinger[5] observed streaks in an electron diffraction investigation of γ crystallites. The streaks were attributed to the inclusion of stacking faults with incorporation of α sequences in the γ chains. Therefore, γ sequences may be present in a matrix of α chains and vice versa. From this, it may be inferred that, after heat treatment of a PVF_2 sample, the α and γ conformations interchange through chain motions. Lovinger[5] proposed other types of more flexible chain motions that are supposed to be more favored than the Takahashi flip-flops, including simultaneous five-bond or seven-bond motions.

A consistent picture of the molecular mechanism may be summarized as follows. Chain motion leading to interchange of G or G′ and T conformations is the first step of the transformation. The second step is the inversion motion proposed by Takahashi et al.[10] to account for the change of polarity of the chains and, thus, the transition of a nonpolar α unit cell into a polar γ cell. In addition, variation of interchain spacing accompanies this motion. They suggested that the segmental flip-flop motion occurs at ca. 423 K and the inversion motion takes place at ca. 443 K.

The conformational approach to the $\alpha \rightarrow \gamma$ transformation gives considerable insight into the process on the molecular level. Bond rotation results in segmental motion of the chain and cooperative motion of the neighboring chains. As a result, the solid-state transformation propagates when the activation energies for these chain motions are overcome at high temperatures. It should be noted that cooperative motion requires regular chain alignment and, therefore, will be impeded by the irregular packing in the amorphous region. This brief review will provide a basis for better understanding of the following discussion on the superstructural aspects of the transformation.

Another important study conducted by Lovinger[6] was based on the observation of the development of superstructures of the α and γ crystallites. It was found that the transformation did not begin until the α and γ spherulites came in contact with each other. Lovinger proposed a mechanism for the solid-state transformation in which the transformation originates at the peripheries of the α spherulites where their lamellae are in contact and collinear with the lamellae of γ spherulites. The rate of transformation decreases as the angle between the lamellae of the α spherulite and the point of contact in the γ spherulite increases toward the perpendicular. Consequently, the transformation propagates along the orientation of the α lamellae toward the nuclei of the α spherulites.

During the course of the longitudinal transformation, the transverse transformation also takes place, resulting in three-dimensional propagation. Lovinger suggested that the transverse transformation was slower due to the amorphous barrier between the lamellae. This conclusion is understandable since the cooperative chain motions require chain alignment, which exists in the lamellae or the longitudinal direction but is deficient in the amorphous layer or the transverse direction. Our data, which will be discussed shortly, provide quantitative support for Lovinger's proposal.

Although the $\alpha \rightarrow \gamma$ transformation has been studied from both the conformational and morphological points of view, the controlling factors in the transformation process are still not clear. A logical proposal is that the structural irregularities may play a role since they would influence a number of morphological features: (1) the energy barrier encountered by the chain motions, (2) the amorphous layers between the lamellae, and (3) the growth of the polymorphs during the crystallization. As such, it is interesting to investigate the effects of structural irregularities on the transformation process.

The influence of structural defects on the rotational energy barrier is probably best resolved by theoretical calculation of the change of the conformational energy along the course of the transformation. Nevertheless, the influence on the interlamellar amorphous layer or the growth of the polymorphs may be investigated by differential scanning calorimetry, as will be shown shortly. The structural defect focused on in this work is the H/H linkage of monomeric units, which has been shown to influence the crystallization of PVF_2.[7] The effect of the molecular weight is also studied since it was also found to influence the crystallization process.[7]

Effect of the Interlamellar Amorphous Phase. It has been reported[6] that the $\alpha \rightarrow \gamma$ transformation may take place at the nuclei of the α spherulites above 435 K. Moreover, as the temperature increases above 438 K, the α chains gain sufficient thermal energy to overcome the energy for the conformational transition to allow the transformation in the interior of the α spherulites. Our experiments were conducted at the lower temperature of 433 K to concentrate on the solid-state transformation initiated at the interface of the α and γ spherulites.

Figure 1 shows the melting endotherm for a Dyflor 2000H sample crystallized at 433 K for 24 h. It is noticed that the α peak starts below the crystallization temperature, T_c. The crystallites responsible for this low-melting α phase must be developed when the temperature of the sample is decreased from T_c prior to the start of a melting scan in the DSC. Warner et al.[11] observed a similar low-melting peak below the crystallization temperature in a study of poly(tetramethylene oxide). They concluded that

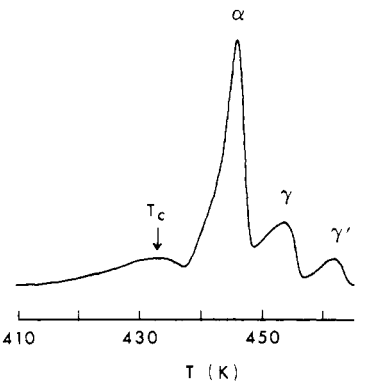

Figure 1. Melting endotherm of Dyflor 2000H crystallized at 433 K for 24 h.

the low-melting peak is due to interlamellar crystallization.

Amorphous material in semicrystalline polymers can be found in both inter- and intraspherulitic regions. Part of the amorphous regions will be crystallized when the temperature is lowered. It is a reasonable assumption that the area of the low-melting α phase is proportional to the content of the interlamellar amorphous regions, which, according to Lovinger,[6] will slow down the transverse propagation of the $\alpha \rightarrow \gamma$ transformation.

In the analysis of a DSC thermogram, the area of the low-melting α phase is separated from the main α peak on the assumption that the latter starts from the crystallization temperature. Then a smooth and continuous curve is constructed for the low-temperature shoulder of the main α peak. The area complementary to the envelope of the main α peak, A_p, is measured and regarded as the area for the low-melting α phase. The peak areas of the α, crystallized γ, and transformed γ phases are also measured and denoted as A_α, A_γ, and $A_{\gamma'}$, respectively. Correlation of the contents of the various phases will provide more information about the $\alpha \rightarrow \gamma$ transformation and allow examination of Lovinger's proposal that transverse propagation across the amorphous boundaries of the lamellae is slower than the longitudinal process.

The peak areas may be grouped in such a way as to represent the degree of transformation and the tendency toward formation of low-melting α crystallites by the interlamellar amorphous phase. Here the heats of fusion for the α and γ polymorphs are assumed to be the same. Since the solid-state transformation does not occur until the two types of spherulites get in contact and the γ' phase originates from the α phase, $(A_\alpha + A_\gamma)$ represents the content of the α phase before the transformation takes place. It follows that $A_{\gamma'}/(A_\alpha + A_\gamma)$ denotes the degree of the $\alpha \rightarrow \gamma$ transformation. The amorphous regions between the crystalline fibrils or lamellae will be well developed when the crystallization is nearly finished and before the transformation begins. Therefore, $A_p/(A_\alpha + A_\gamma)$ represents the amount of the low-melting α crystallites developed per unit of the original melt-crystallized α crysallites.

$A_{\gamma'}/(A_\alpha + A_\gamma)$ is plotted against $A_p/(A_\alpha + A_\gamma)$ in Figure 2 to show the relation between the degree of transformation and the content of the interlamellar amorphous regions. The data are somewhat scattered. However, an interesting correlation is observed if the data are parameterized by the percentage of the crystallized γ phase in the overall crystalline regions, denoted by the quantity $A_\gamma/(A_\alpha + A_\gamma + A_{\gamma'})$. A_p is not included in the denominator because the low-melting α phase does not exist when the $\alpha \rightarrow \gamma$ transformation proceeds at high temperatures. For the groups in which the percentages of the crystallized γ phase are about 2% and 5%, respectively, the degree of

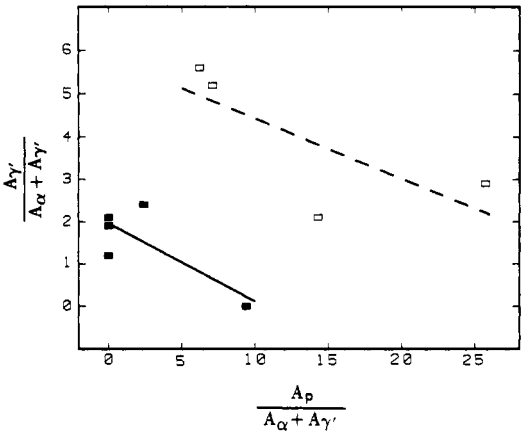

Figure 2. Dependence of the degree of the $\alpha \rightarrow \gamma$ transformation on the content of the interlamellar amorphous phase for PVF_2 samples crystallized at 433 K for 24 h: (■) $A_{\gamma'}/(A_\alpha + A_\gamma + A_{\gamma'})$ = 0.8–2.6; (□) $A_{\gamma'}/(A_\alpha + A_\gamma + A_{\gamma'})$ = 4.7–5.6.

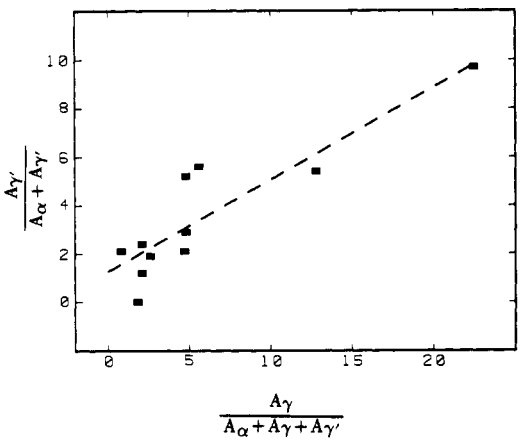

Figure 3. Dependence of the degree of the $\alpha \rightarrow \gamma$ transformation on the percentage of the γ spherulites in the crystalline regions for PVF_2 samples crystallized at 433 K for 24 h.

the solid-state transformation decreases with the interlamellar amorphous content. This verifies Lovinger's proposal[6] that the solid-state transformation is retarded by the amorphous barrier. It is noted that, as the percentage of the crystallized γ phase of a group increases from 2% to 5%, the conversion increases. Therefore, the degree of transformation is also a function of the percentage of the crystallized γ phase in the crystalline regions.

Effect of the γ Spherulites. According to Lovinger,[6] the solid-state transformation would be expected to be initiated at the interface of the α and γ spherulites at 433 K, the temperature of these experiments. Thus, the process should be enhanced by the γ crystallites since large or more γ spherulites will result in more initiation sites along their peripheries and, thus, a higher degree of transformation. Indeed, the degree of the $\alpha \rightarrow \gamma$ transformation is an increasing function of the percentage of the crystallized γ phase in Figure 3.

It should be noted that the transformation increases with the content of the crystallized γ phase despite the inverse effect of the interlamellar amorphous phase discussed in the last section. It is important to note that the transformation does not appear to be a decreasing function of the interlamellar amorphous content unless the influence of the γ spherulites is separated. Therefore, it may be argued that the presence of the γ spherulite is a stronger factor than the interlamellar amorphous phase in the transformation process. The main effect of the γ spherulite is to initiate the longitudinal propagation, whereas the amorphous layer only affects the transverse propaga-

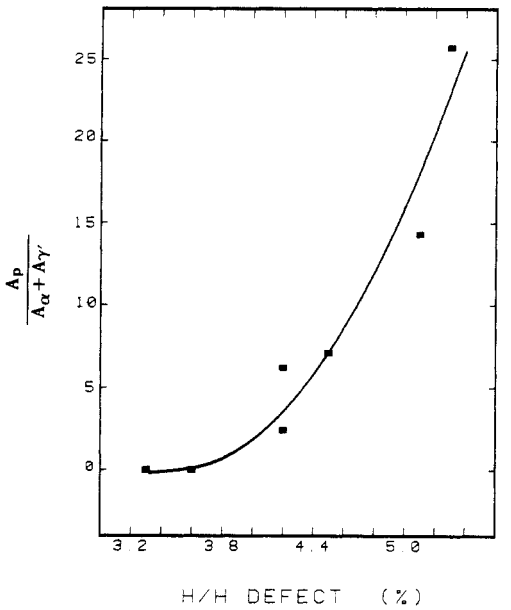

Figure 4. Dependence of the content of the interlamellar amorphous phase on the H/H defect content for PVF_2 samples crystallized at 433 K for 24 h.

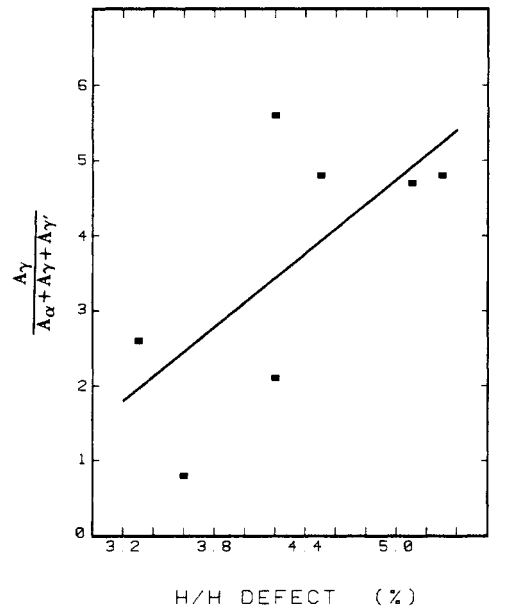

Figure 5. Dependence of the percentage of the γ spherulites in the crystalline regions on the H/H defect content for PVF_2 samples crystallized at 433 K for 24 h.

tion. The observation that the γ spherulites have a larger effect than the interlamellar amorphous layer is again consistent with Lovinger's proposal that the longitudinal propagation is faster than the transverse one.

Effect of the Head-to-Head Defect. Since the γ spherulites and the interlamellar amorphous layer are found to be important factors, it is of interest to investigate whether the H/H defect will exert its influence on the transformation process through the two factors. The relation between the interlamellar amorphous content and the H/H defect at 433 K with the molecular weight in the range of 94 000–186 000 is illustrated in Figure 4. The content of the interlamellar amorphous phase increases dramatically with the H/H defect percentage. Therefore, the H/H defect would be expected to have a retarding effect on the $\alpha \rightarrow \gamma$ transformation if its influence on the percentage of the γ crystallites in crystalline regions were not considered.

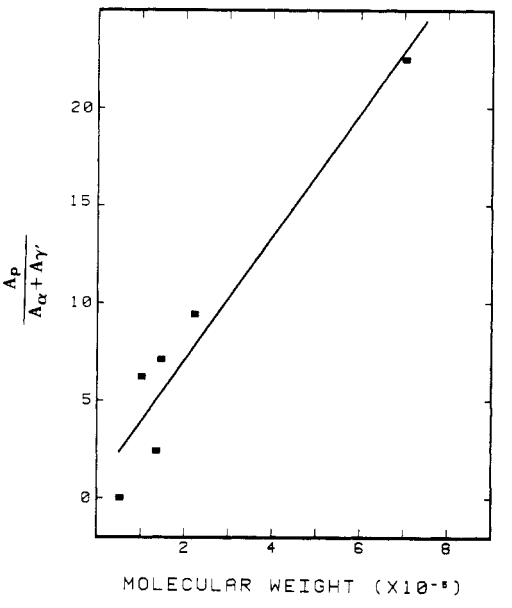

Figure 6. Dependence of the content of the interlamellar amorphous phase on the molecular weight for PVF_2 samples crystallized at 433 K for 24 h.

However, the H/H defect may also influence the competitive growth of the polymorphs. Figure 5 shows the dependence of the percentage of γ spherulites on the H/H defect content at 433 K for the same samples shown in Figure 4. Despite the scatter in the data, which may arise from effects of molecular weight and other structural defects, a trend in which $A_\gamma/(A_\alpha + A_\gamma + A_{\gamma'})$ increases with the H/H defect percentage is seen. Therefore, considered in isolation from the effect of H/H defect on the amorphous content described above, increasing the H/H defect concentration would be expected to enhance the transformation. Since the γ spherulites and the interlamellar amorphous layer have opposing influences on the $\alpha \rightarrow \gamma$ transformation and because the two competing factors are both enhanced by the reversed monomer linkage, the effect of the H/H defect on the $\alpha \rightarrow \gamma$ transformation is obviously complex.

Effect of the Molecular Weight. The interlamellar amorphous content for crystallization at 433 K and the H/H defect concentration in the range of 4.0–4.5% is correlated with the molecular weight in Figure 6. The content of the interlamellar amorphous phase appears to increase with the molecular weight. In previous work, the degree of crystallinity of PVF_2 was found to decrease with the molecular weight in this temperature range.[7,9] Hence, it is natural that the amorphous phase should become richer as the molecular weight increases.

The correlation of the percentage of γ crystallites with the molecular weight at 433 K for the same samples shown in Figure 6 is illustrated in Figure 7. Although more data in the molecular weight range 300 000–600 000 would certainly help clarify the relation, it seems that $A_\gamma/(A_\alpha + A_\gamma + A_{\gamma'})$ increases with the molecular weight. As in the case of the H/H defect, both of the competing factors in the transformation—γ spherulites and the amorphous layer—are enhanced by higher molecular weight. Therefore, the effects of the molecular weight on the transformation are again twofold. As a result, the correlation between the degree of transformation and the molecular weight is also complicated.

Summary

The $\alpha \rightarrow \gamma$ transformation is enhanced by the γ spherulites at 433 K because the chance of initiating the

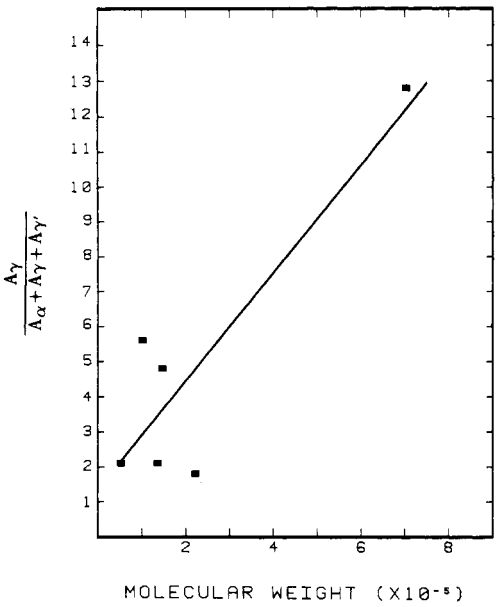

Figure 7. Dependence of the percentage of the γ spherulites in the crystalline regions on the molecular weight for PVF_2 samples crystallized at 433 K for 24 h.

longitudinal propagation is increased. On the other hand, the transformation is impeded by the interlamellar amorphous phase, which acts as a barrier to the transverse propagation. Both the percentage of the γ spherulites in the crystalline regions and the content of the interlamellar amorphous phase increase with the head-to-head defect concentration and the molecular weight. As a result, the degree of the $\alpha \rightarrow \gamma$ transformation appears to be a complicated function of both of these molecular parameters.

Acknowledgment. This work was supported by the Polymers Program of the Office of Naval Research.

Registry No. PVF_2, 24937-79-9.

References and Notes

(1) Lovinger, A. J. *Dev. Crst. Polym.* **1982**, *1*, 195.
(2) Gianotti, G.; Capizzi, A.; Zamboni, V. *Chim. Ind. (Milan)* **1973**, *55*, 501.
(3) Prest, W. M.; Luca, P. J. *J. Appl. Phys.* **1975**, *46*, 4136.
(4) Takahashi, Y.; Tadokoro, H. *Macromolecules* **1980**, *13*, 1316.
(5) Lovinger, A. J. *J. Appl. Phys.* **1981**, *52* (10), 5934.
(6) Lovinger, A. J. *Polymer* **1980**, *21*, 1318.
(7) Chen, L. T.; Frank, C. W. *Ferroelectrics* **1984**, *57*, 51.
(8) Morra, B. S.; Stein, R. S. *J. Polym. Sci., Polym. Phys. Ed.* **1982**, *20*, 2243.
(9) Watkins, K.; Bowker, S. M.; Frank, C. W., submitted to *Macromolecules*.
(10) Takahashi, Y.; Matsubara, Y.; Tadokoro, H. *Macromolecules* **1982**, *15*, 334.
(11) Warner, F. P.; Brown, D. S.; Wetton, R. E. *Polymer* **1981**, *22*, 1349.
(12) Sanchez, I. C.; Eby, R. K. *J. Res. Natl. Bur. Stand., Sect. A* **1973**, *77A*, 353.
(13) Hoffman, J. D.; Weeks, J. J. *J. Res. Natl. Bur. Stand., Sect. A* **1962**, *66A*, 13.

Structural Inhomogeneities in the Range 2.5–2500 Å in Polyacrylamide Gels

Anne-Marie Hecht,† Robert Duplessix,‡ and Erik Geissler*†

Laboratoire de Spectrométrie Physique,§ F-38402 St. Martin d'Hères Cedex, France, and CRM, F-67083 Strasbourg Cedex, France. *Received February 13, 1985*

ABSTRACT: Measurements are presented of the scattering function $S(Q)$ from poly(acrylamide-*co*-bisacrylamide) copolymer gels using light (SLS), small-angle neutron (SANS), and small-angle X-ray (SAXS) scattering. The gels had a fixed acrylamide content (0.08 g/mL) and a bisacrylamide content that varied between 0 and 0.005 g/mL. It is found that all three sets of data can be spliced together to form a single continuous scattering function $S(Q)$, where the scattering wave vector Q lies in the range $4 \times 10^4 \leq Q \leq 1.5 \times 10^7$ cm^{-1}. Contrast variation SANS data show that the spectra can be separated into two parts. The first, a homogeneous solution, gives rise to a quasi-Lorentzian signal with a correlation length ξ that increases with increasing bisacrylamide content. The behavior of $S(Q)$ at high Q values shows that the value of the radius of cross section r_0 of the polymer chains in this phase increases from about 2.5 to 4 Å with increasing bisacrylamide. The total polymer content in this phase is found, however, to be approximately constant. In addition to this homogeneous spectrum, there is also excess forward scattering arising from an inhomogeneous component in the gel, which is characterized by concentration fluctuations of large amplitude. Because of the continuity of $S(Q)$ with the light scattering curves, $S(Q)$ can be calibrated, and one can hence obtain the contribution to the invariant $M_2^{tot} = \int_0^\infty S(Q)Q^2\,dQ$, which is caused by the heterogeneities. Furthermore, in the SANS region of the spectra, the curves follow a fractal behavior, the dimensionality of which is variable at will—by suitable choice of the bisacrylamide content—between 0 and 3.

Introduction

In contrast to polymer solutions, most gels are inhomogeneous structures. The degree of inhomogeneity depends upon the way in which the gel has been formed, and the ultimate strength of these materials is sensitively dependent on such defects. In certain cases, the mechanical properties can be notably enhanced by the artificial introduction of extraneous inhomogeneities, such as silica filler in silicone rubbers. The presence of cross-linking inhomogeneities, on the other hand, promotes brittleness, which for many mechanical applications, is an undesirable characteristic in rubbers.

The effect of cross-linking inhomogeneities on such properties as the permeability of polyacrylamide gels has

† Laboratoire de Spectrométrie Physique.
‡ CRM.
§ CNRS associate laboratory.

0024-9297/85/2218-2167$01.50/0